taxonomy

MDPI

Article

Acinetobacter nematophilus sp. nov., *Alcaligenes nematophilus* sp. nov., *Enterobacter nematophilus* sp. nov., and *Kaistia nematophila* sp. nov., Isolated from Soil-Borne Nematodes and Proposal for the Elevation of *Alcaligenes faecalis* subsp. *faecalis*, *Alcaligenes faecalis* subsp. *parafaecalis*, and *Alcaligenes faecalis* subsp. *phenolicus* to the Species Level

Ricardo A. R. Machado [1,*], Ameni Loulou [2,†], Aashaq Hussain Bhat [1,†], Maristella Mastore [3], Céline Terrettaz [4], Maurizio Francesco Brivio [3] and Sadreddine Kallel [2,*]

[1] Experimental Biology Research Group, Institute of Biology, University of Neuchâtel, 2000 Neuchâtel, Switzerland
[2] Laboratory of Bio-aggressor and Integrated Protection in Agriculture, Department of Plant Health and Environment, National Agronomic Institute of Tunisia, University of Carthage, Tunis-Mahrajène 1082, Tunisia
[3] Laboratory of Comparative Immunology and Parasitology, Department of Theoretical and Applied Sciences, University of Insubria, 21100 Varese, Italy
[4] Laboratory of Microbiology, Institute of Biology, University of Neuchâtel, 2000 Neuchâtel, Switzerland
* Correspondence: ricardo.machado@unine.ch (R.A.R.M.); kallel.sadreddine@gmail.com (S.K.)
† These authors contributed equally to this study.

Citation: Machado, R.A.R.; Loulou, A.; Bhat, A.H.; Mastore, M.; Terrettaz, C.; Brivio, M.F.; Kallel, S. *Acinetobacter nematophilus* sp. nov., *Alcaligenes nematophilus* sp. nov., *Enterobacter nematophilus* sp. nov., and *Kaistia nematophila* sp. nov., Isolated from Soil-Borne Nematodes and Proposal for the Elevation of *Alcaligenes faecalis* subsp. *faecalis*, *Alcaligenes faecalis* subsp. *parafaecalis*, and *Alcaligenes faecalis* subsp. *phenolicus* to the Species Level. *Taxonomy* **2023**, *3*, 148–168. https://doi.org/10.3390/taxonomy3010012

Received: 19 November 2022
Revised: 17 February 2023
Accepted: 24 February 2023
Published: 9 March 2023

Abstract: Four bacterial strains, A-IN1^T, A-TC2^T, E-TC7^T, and K-TC2^T, isolated from soil-borne nematodes of the species *Oscheius tipulae* and *Acrobeloides bodenheimeri*, were found to represent new species of the genera *Acinetobacter*, *Alcaligenes*, *Enterobacter*, and *Kaistia*, respectively. In this study, we described these new species using a polyphasic taxonomic approach that included whole-genome and whole-proteome phylogenomic reconstructions, core genome sequence comparisons, and phenotypic characterization. Phylogenomic reconstructions using whole-genome and whole-proteome sequences show that A-IN1^T is closely related to *Acinetobacter guillouiae* DSM 590^T and to *Acinetobacter bereziniae* LMG 1003^T. The dDDH values between A-IN1^T and these latest strains are 25.1 and 39.6%, respectively, which are below the 70% divergence threshold for prokaryotic species delineation. A-TC2^T is closely related to *Alcaligenes faecalis* subsp. *faecalis* DSM 30030^T and to *Alcaligenes faecalis* subsp. *phenolicus* DSM 16503^T. The dDDH values between A-TC2^T and these latest strains are 47.0 and 66.3%, respectively. In addition, the dDDH values between *Alcaligenes faecalis* subsp. *faecalis* DSM 30030^T, *Alcaligenes faecalis* subsp. *phenolicus* DSM 16503^T, and *Alcaligenes faecalis* subsp. *parafaecalis* are always lower than 70%, demonstrating that the three strains represent species within the genus *Alcaligenes* rather than subspecies within *Alcaligenes faecalis*. E-TC7^T is closely related to *Enterobacter kobei* DSM 13645^T, *Enterobacter chuandaensis* 090028^T, and to *Enterobacter bugandensis* STN0717-56^T. The dDDH values between E-TC7^T and these strains are 43.5, 42.9, and 63.7%, respectively. K-TC2^T is closely related to *Kaistia terrae* DSM 21341^T and to *Kaistia defluvii* JCM 18034^T. The dDDH values between these strains are 29.2 and 30.7%, respectively. Several biochemical tests allow to differentiate the type strains of the newly described species from the type strains of their more closely related species. Based on the results of this polyphasic taxonomic approach, the following new species are proposed: *Acinetobacter nematophilus* sp. nov. with A-IN1^T (=CCM 9231^T =CCOS 2018^T) as the type strain, *Alcaligenes nematophilus* sp. nov. with A-TC2^T (=CCM 9230^T =CCOS 2017^T) as the type strain, *Enterobacter nematophilus* sp. nov. with E-TC7^T (=CCM 9232^T =CCOS 2020^T) as the type strain, and *Kaistia nematophila* sp. nov. with K-TC2^T (=CCM 9239^T =CCOS 2022^T) as the type strain. In addition, we propose the elevation of *Alcaligenes faecalis* subsp. *faecalis*, *Alcaligenes faecalis* subsp. *parafaecalis*, and *Alcaligenes faecalis* subsp. *phenolicus* to the species level. Therefore, we propose the creation of *Alcaligenes parafaecalis* sp. nov. with DSM 13975^T as the type strain, and *Alcaligenes phenolicus* sp. nov. with DSM 16503^T as the type strain. Our study contributes to a

better understanding of the biodiversity and phylogenetic relationships of bacteria associated with soil-borne nematodes.

Keywords: soil-borne nematodes; nematophilic bacteria; novel bacterial species; taxonomic description

1. Introduction

Soil nematodes associate with several different bacterial species [1–3]. Certain nematodes, for instance, establish obligate mutualistic associations with entomopathogenic bacteria, which aid them to kill insects by producing toxins and digestive enzymes [4,5]. Apart from this, bacteria can also serve as food sources for free-living nematodes, aid nematodes in development, defense, reproduction and nutrient acquisition [1,2,6–12]. Bacteria thus play essential roles for soil-borne nematodes.

To characterize the biodiversity of bacteria associated with soil-borne nematodes, we often conduct surveys to recover soil nematodes, culture them in the laboratory, and then isolate their associated bacteria. During one of our surveys, we isolated several nematode species, which harbor four novel bacterial species of the genus *Acinetobacter*, *Alcaligenes*, *Enterobacter*, and *Kaistia* [13–15]. In this study, we morphologically, biochemically and molecularly characterized them to describe these new species.

The genus *Acinetobacter* was first described by Brisou and Prévot (1954) [16]. Members of this genus are Gram-negative coccobacilli, non-motile, non-spore-forming, aerobic, and mesophilic. Bacteria of this genus can survive under different environmental conditions and have been isolated from food, including fish, meat, cheese, milk, and vegetables [17]. Moreover, some *Acinetobacter* species have been recovered from activated sludge, sewage, dump sites, raw wastewater, and hydrocarbon-contaminated areas [18–20]. Over the past decades, some species of this genus have emerged as significant nosocomial and opportunistic pathogens causing outbreaks of colonization and infection, especially in immunosuppressed patients [21,22]. At the time of writing, this genus includes 76 species with valid published and correct names (https://lpsn.dsmz.de/genus/acinetobacter; accessed on 3 March 2023).

The genus *Alcaligenes* was first described by Castellani and Chalmers (1919) [23]. Members of this genus are Gram-negative, coccobacillary rods, motile, aerobic, and mesophilic. Bacteria of this genus have been isolated from plants, soil, sediment, bioprocess residues, water, and clinical samples [24–26]. Some species are resistant to heavy metals such as chromium, and other environmental pollutants such as phenol [24,27,28]. At the time of writing, this genus includes four species and three subspecies with valid published and correct names (https://lpsn.dsmz.de/genus/alcaligenes; accessed on 3 March 2023).

The genus *Enterobacter* was first described by Hormaeche and Edwards (1960) [29]. Members of this genus are Gram-negative, rod-shaped, non-spore forming, facultative anaerobic, and mesophilic [30]. Bacteria of this genus are widely distributed in nature. They are plant pathogens, colonize the human gut, and certain species can also cause urinary and respiratory infections in humans [31–35]. At the time of writing, this genus includes 24 species with valid published names (https://lpsn.dsmz.de/genus/enterobacter; accessed on 3 March 2023). Noteworthily, this latest list still does not reflect recent propositions to elevate the following subspecies to the species level: *E. cloacae* subsp. *cloacae*, *E. cloacae* subsp. *dissolvens*, *E. hormaechei* subsp. *hormaechei*, and *E. hormaechei* subsp. *xiangfangensis* [36]. All these species are actually independent species rather than subspecies: *E. cloacae*, *E. dissolvens*, *E. hormaechei*, and *E. xiangfangensis* [36].

The genus *Kaistia* was first described by Im et al. (2005) [37]. Members of this genus are Gram-negative, short rod to coccus-shaped, non-motile, predominantly aerobic although some species can be facultative anaerobes, and mesophilic [37]. They are also widely distributed in nature. Some species have been isolated from peat layers, anaerobic sludge blankets, soil sediments, freshwater, and sediment contaminated with sewage [38–43]. At

the time of writing, this genus includes nine species with valid published and correct names (https://lpsn.dsmz.de/genus/kaistia; accessed on 3 March 2023).

In this study, we characterized four bacterial strains that represent four novel species for which we propose the following names: *Acinetobacter nematophilus* sp. nov., *Alcaligenes nematophilus* sp. nov., *Enterobacter nematophilus* sp. nov., and *Kaistia nematophila* sp. nov. In addition, we propose the elevation of *Alcaligenes faecalis* subsp. *faecalis*, *Alcaligenes faecalis* subsp. *parafaecalis*, and *Alcaligenes faecalis* subsp. *phenolicus* to the species level. Therefore, we propose the creation of the following new species: *Alcaligenes parafaecalis* sp. nov., and *Alcaligenes phenolicus* sp. nov. Our study, therefore, contributes to a better understanding of the biodiversity and phylogenetic relationships of bacteria associated with soil-borne nematodes.

2. Material and Methods

2.1. Bacteria Isolation

Bacterial strains were obtained from different soil-borne nematode strains isolated at different locations in Tunisia using the soil baiting method and different insects as baits [44] as described elsewhere [13]. This procedure was carried out to isolate entomophilic nematodes. *Acinetobacter nematophilus* sp. nov. A-IN1^T was isolated from an unidentified soil-borne nematode, IN1, collected in the National Agronomic Institute of Tunisia (Tunis, Tunisia). These nematodes were isolated using *Galleria mellonella* larvae as baits. Unfortunately, we were unsuccessful in establishing long-term nematode colonies under laboratory conditions, and we could not identify these nematodes. However, insects presented typical symptoms of *Heterorhabditis* nematode infestation such as that the nematodes turned red within 48 h upon nematode inoculation. *Alcaligenes nematophilus* sp. nov. A-TC2^T and *Kaistia nematophila* sp. nov. K-TC2^T were isolated from *Oscheius tipulae* TC2 nematodes collected in Takilsa (Cap Bon, Tunisia). These nematodes were isolated using *Ceratitis capitata* pupae as baits. *Enterobacter nematophilus* sp. nov. E-TC7^T was isolated from *Acrobeloides bodenheimeri* TC7 nematodes collected in Takilsa (Cap Bon, Tunisia). These nematodes were isolated using *Ceratitis capitata* pupae as baits. To isolate the bacteria from *O. tipulae* TC2 and *A. bodenheimeri* TC7 nematodes, approximately 200 specimens of each nematode strain were washed several times with sterile phosphate buffered saline (PBS, 1mM KH_2PO_4, 1mM K_2HPO_4, 5M NaCl, pH 7.2). Then, the nematodes were incubated in a 1% v/v sodium hypochlorite/PBS solution for 5 min under gentle orbital agitation. After this incubation period, the nematodes were recovered by decanting, washed with sterile PBS, and incubated again in a 1% v/v sodium hypochlorite/PBS solution. After this incubation period, the nematodes were again recovered by decanting, washed several times with PBS and sonicated in sterile PBS at 4 °C for 30 sec and at 100W burst using an ultrasonic processor (Labsonic-L, B-Braun Biotech Inc, Allentown, PA, USA). The nematode body fragments were pelleted by centrifugation at 650× g (10 min, 4 °C). Then, 100 µL of supernatants were cultured in lysogeny broth (LB) medium overnight at 30 °C under constant shaking (180 rpm). An aliquot of the resulting cultures was plated on LB agar medium and incubated at 30 °C for 24–48 h. Single colonies were sub-cultured and used for further experiments. To isolate the bacteria from IN1 nematodes, a few drops of hemolymph from *G. mellonella* larvae infested with these nematodes were cultured in LB medium. To this end, the larvae were dipped first in 70% ethanol, and then punctured with a sterile needle in the ventral part. The released hemolymph was cultured in LB medium and incubated overnight at 30 °C for 24 h under constant shaking (180 rpm). An aliquot of the resulting cultures was plated on LB agar medium and incubated at 30 °C for 24–48 h. Single colonies were sub-cultured and used for further experiments. Different procedures such as the characterization of colony and cell morphology, and 16S rRNA gene sequencing were carried out to determine culture purity. The bacteria were deposited in the Czech Collection of Microorganisms (CCM) and in the national Culture Collection of Switzerland (CCOS) under the following accession numbers: *Acinetobacter nematophilus* A-IN1^T (=CCM 9231^T =CCOS 2018^T), *Alcaligenes nematophilus* A-TC2^T (=CCM 9230^T =CCOS 2017^T), *Enterobacter*

nematophilus E-TC7^T (=CCM 9232^T =CCOS 2020^T), and *Kaistia nematophila* K-TC2^T (=CCM 9239^T =CCOS 2022^T).

2.2. Bacteria Molecular Characterization

To molecularly characterize the newly isolated bacterial strains, phylogenetic and phylogenomic relationships were reconstructed using 16S rRNA gene, whole-genome and whole-proteome sequences. In addition, sequence similarity scores were calculated as described below.

2.3. 16S rRNA Gene Sequencing

To obtain 16S rRNA gene sequences, the 16S rRNA gene was amplified by polymerase chain reaction (PCR) using the following universal primers: 27F (5'-AGAGTTTGATCMTGG CTCAG-3') and 1525R (5'-AAGGAGGTGWTCCARCC-3'). The following cycling conditions were used: 1 cycle at 94 °C for 10 min followed by 40 cycles at 94 °C for 60 s, 55 °C for 60 s, 72 °C for 60 s and a final extension at 72 °C for 5 min [3,45,46]. PCR products were separated by electrophoresis in a 1% TAE-agarose gel stained with GelRed nucleic acid gel stain (Biotium), gel-purified (QIAquick Gel Purification Kit, Qiagen) and sequenced by Sanger sequencing (Microsynth AG, Balgach, Switzerland). The obtained sequences were manually curated using Bioedit 7.2.5 [47]. In addition, 16S rRNA gene sequences were obtained directly from the whole-genome sequences using the bacterial ribosomal RNA predictor Barrnap 0.7 using the following parameters: reject length threshold = 0.5; length cutoff= 0.8; and e-value= 0.00001 [48]. The obtained sequences were identical to those obtained by Sanger sequencing. Phylogenetic relationships were reconstructed using the Maximum Likelihood method based on the Kimura 2-parameter model in MEGA7 as described above [49–51]. Tree support was determined by the bootstrap method based on 100 replicates. Graphical representation and edition of the trees were performed with Interactive Tree of Life (v3.5.1) [52,53]. The National Center for Biotechnology Information (NCBI) accession numbers of the sequences used for these analyses are shown in Table S1.

2.4. Whole Genome Sequencing

Genome sequences were obtained as described elsewhere [54,55]. Briefly, genomic DNA was extracted and purified using the GenElute Bacterial Genomic DNA Kit (Sigma–Aldrich, Switzerland) following the manufacturer's instructions. The resulting DNA was used for library preparation using the TruSeq DNA PCR–Free LT Library Prep (FC–121–3003) kit. Indexed libraries were then pooled at equimolar concentrations and sequenced (2 × 150 bp) on an Illumina HiSeq 3000 instrument. Genomes were assembled using the Bactopia pipeline [56]. To this end, the raw Illumina reads were quality trimmed using Trimmomatic 0.39 [57]. The resulting reads were assembled with SPAdes 3.14.1 [58]. Scaffolds with a mean read–depth smaller than 20% of the median read–depth of the longer scaffolds ($\geq$5000 bp) as well as scaffolds that were shorter than 200 bp were removed. Minor assembly errors were corrected using Pilon 1.22 with default parameters [59]. Completeness and contamination of the assembled genomes was assessed using checkM v1.1.6 with default parameters [60].

2.5. Whole Genome and Whole Proteome-Based Phylogenies

To reconstruct whole genome-based phylogenies, genomes were first aligned using Roary 3.13.0. Genes to be considered core had to be present in 85% of the genomes with an 85% protein identity and a coverage higher than 90%. Obtained alignments were used to build phylogenomic trees using FastTree 2.1.10 based on the Generalized Time Reversible Model (GTR) [61]. Branch support was assessed using the Shimodaira-Hasegawa-like procedure based on 100 replicates [61]. To reconstruct whole proteome-based phylogenies, first all ORFs from all genomes were extracted using Prodigal [62]. Then, homologous genes (85% or higher similarity, and a coverage higher than 90%) were clustered using MMSEQS2 (e-value: 0.001, sensitivity: 7.5, and cover: 0.5) and

MCL (Inflation = 2) [63–65]. Orthologous genes were then translated and aligned using MAFFT [66]. Orthologous genes had to be present in more than 85% of the genomes to be considered core. Lastly, a maximum-likelihood-based phylogenomic tree was reconstructed based on the inferred core-proteome alignment using RAxML [67,68]. Branch support was assessed using the rapid bootstrap method based on 100 replicates [69]. Graphical representation and editing of the trees were performed with the Interactive Tree of Life (v3.5.1) [52,53]. Whole-genome sequence similarities were calculated by the GBPD (Genome Blast Distance Phylogeny) method using the Genome-to-Genome Distance Calculator 2.1 and formula 2 of the Deutsche Sammlung von Mikroorganismen und Zellkulturen (DSMZ) web service (http://ggdc.dsmz.de; accessed 5 June 2022) using default parameters [70–73]. The NCBI accession numbers of the sequences used for these analyses are shown in Table S1.

2.6. Physiological, Biochemical and Morphological Characterization

To physiologically, biochemically, and morphologically characterize the newly isolated bacterial strains, bacterial cultures from single colonies were used. Cell morphology was observed under a Leica DM4 B optical microscope at 1000× magnification, with cells grown for 16 h at 28 °C on LB. Pictures were taken using a built-in camera (Leica DFC7000T). The optimum temperature for bacterial growth was evaluated on LB agar medium at 20 °C, 24 °C, 30 °C, 32 °C, 37 °C, and 42 °C. Growth on medium containing different salt concentrations and pH was evaluated in 3 mL of LB medium, using 15-mL Falcon tubes. Five NaCl concentrations were used: 1% (Regular LB medium), 2%, 3%, 5% and 7%. Five different pH were used: 3, 5, 7, 8, and 9. Each tube was inoculated with 0.1 mL of an overnight bacterial culture, then incubated for 24 h at 28 °C and 180 rpm. Three tubes per treatment were considered. Cytochrome oxidase production was tested on discs containing *N,N*-dimethyl-p-phenylenediamine oxalate and α-naphthol (Sigma-Aldrich, Switzerland). Catalase activity was determined by adding a drop of 10% (*v*/*v*) H_2O_2 into 50 µL of a 16 h-old bacterial culture. Biochemical characterization was carried out using the API20E (bioMérieux, Inc. Durham, NC, USA) according to the manufacturer's instructions. To this end, bacteria were grown for 16h at 28 °C in LB agar Petri plates. Then, one single colony was re-suspended in 5 mL of 0.85% NaCl. The resulting bacterial solution was used to inoculate the different microtubes containing the biochemical tests. Samples were incubated at 28 °C. Results were evaluated after 24 h. Gram staining was carried out using the Gram-Color modified (phenol-free) staining kit following the manufacture's instructions (Sigma–Aldrich, Buchs, Switzerland). Cell morphology, optimum temperature for bacterial growth, growth on medium containing different salt concentrations and pH, and Gram reaction were evaluated only in the novel species described in this study. Biochemical tests such as cytochrome oxidase production, catalase activity, and the API20E tests were evaluated, in parallel, two independent times. The reference bacterial strains were obtained from the Korean agricultural culture collection (KACC), the German Collection of Microorganisms and Cell Cultures (DSMZ), the Czechoslovak National Collection of Type Cultures (CNCTC), and the Japan Collection of Microorganisms (JCM) as described in Table S5.

3. Results and Discussion

3.1. Phylogenetic and Phylogenomic Reconstructions and Sequence Comparisons

Phylogenetic reconstructions based on 16S rRNA gene sequences show that A-IN1^T is more closely related to *Acinetobacter bereziniae* LMG 1003^T (Figure S1A). The 16S rRNA gene sequence similarity score between A-IN1^T and this strain is 99.4% (Figure S1B). Based on phylogenies reconstructed from core-genome and core-proteomes, A-IN1^T is more closely related to *A. bereziniae* LMG 1003^T (Figure 1 and Figure S5A). The phylogenetic tree obtained in this study largely resembles the trees obtained in previous studies [74,75]. The digital DNA-DNA hybridization (dDDH) score between A-IN1^T and this strain is 39.6% (Table 1). These values are below the 70% divergence threshold for prokaryotic species delineation [70,72,76].

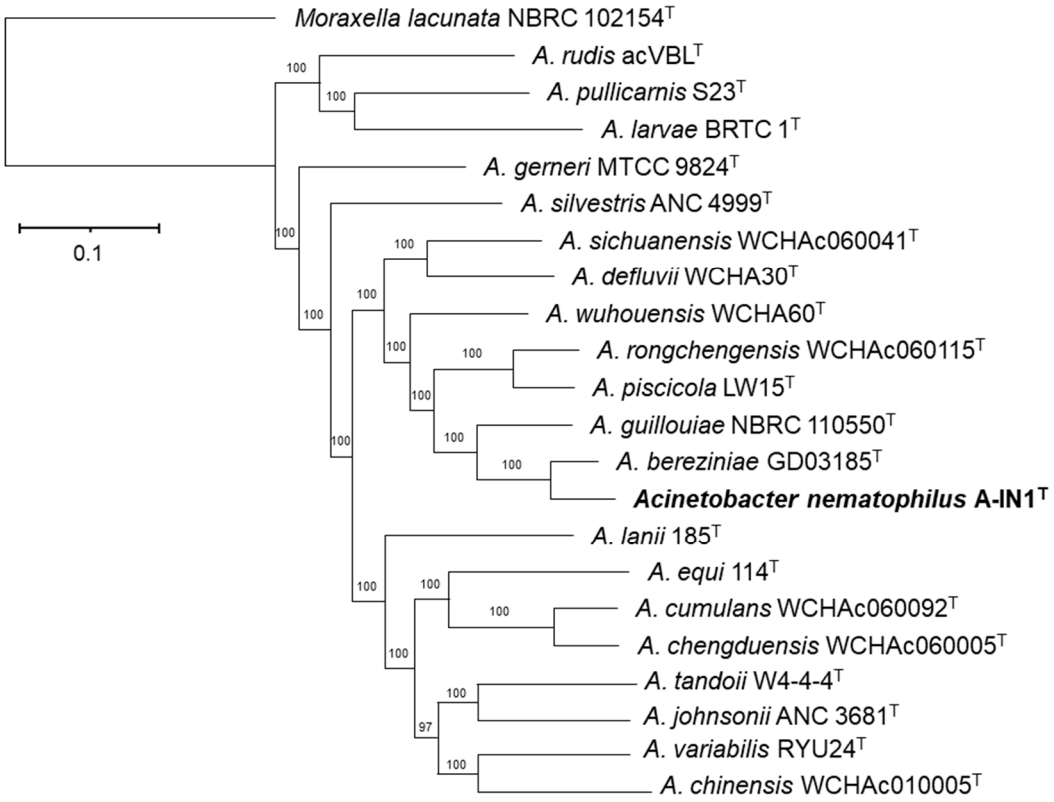

Figure 1. Phylogeny based on core genome sequences of several species of the genus *Acinetobacter*. 644754 nucleotide positions (601 core genes) were used in the analyses. Numbers at the nodes represent SH-like branch supports. Phylogenomic trees were built using FastTree 2.1.10 based on the Generalized Time Reversible Model (GTR) [61]. Accession numbers of the sequences used in the analyses are shown in Table S1. Bold indicates a novel taxonomic proposal.

Phylogenetic reconstructions based on 16S rRNA gene sequences show that A-TC2^T clusters together with *Alcaligenes faecalis* subsp. *faecalis* DSM 30030^T (Proposed name: *Alcaligenes faecalis*) and *A. faecalis* subsp. *phenolicus* DSM 16503^T (Proposed name: *Alcaligenes phenolicus*) (Figure S2A). The 16S rRNA gene sequence similarity scores between A-TC2^T and these latest strains are 99.8% in both cases (Figure S2B). Based on phylogenies reconstructed from core-genome and core-proteomes, A-TC2^T is more closely related to *A. faecalis* subsp. *phenolicus* DSM 16503^T (Proposed name: *Alcaligenes phenolicus*) (Figures 2 and S5B). Previous taxonomic studies have not included core-genome phylogenies to compare [26,27]. The digital DNA–DNA hybridization (dDDH) score between A-TC2^T and this strain is 66.3% (Table 2). This value is below the 70% divergence threshold for prokaryotic species delineation [70,72,76]. In addition, we observed that dDDH scores between *A. faecalis* subsp. *faecalis* DSM 30030^T (Proposed name: *Alcaligenes faecalis*), *A. faecalis* subsp. *parafaecalis* DSM 13975^T (Proposed name: *Alcaligenes parafaecalis*) and *A. faecalis* subsp. *phenolicus* DSM 16503^T (Proposed name: *Alcaligenes phenolicus*) are always below 70%, demonstrating that these three strains represent species rather than subspecies (Table 2).

Table 1. Pairwise comparison of digital DNA-DNA Hybridization (dDDH) scores (%) of several species of the genus *Acinetobacter*. Accession numbers of the sequences used in the analyses are shown in Table S1. Colors indicate the degree of relatedness between bacterial species pairs.

	A. rudis DSM 24031^T	*A. pullicarnis* S23^T	*A. larvae* BRTC-1^T	*A. gerneri* MTCC 9824^T	*A. silvestris* ANC 4999^T	*A. sichuanensis* WCHAc060041^T	*A. defluvii* WCHA30^T	*A. wuhouensis* WCHA60^T	*A. rongchengensis* WCHAc060115^T	*A. piscicola* LW15^T	*A. guillouiae* DSM 590^T	*A. bereziniae* LMG 1003^T	*A. nematophilus* sp. nov. A-IN1^T	*A. lanii* 185^T	*A. equi* 114^T	*A. cumulans* WCHAc060092^T	*A. chengduensis* WCHAc060005^T	*A. tandoii* DSM 14970^T	*A. johnsonii* DSM 69633^T	*A. variabilis* NIPH 2171^T	*A. chinensis* WCHAc010005^T
A. rudis DSM 24031^T	ID	21.2	22.0	21.9	20.9	21.3	21.4	21.7	21.0	21.3	21.5	21.7	20.8	21.4	21.5	21.3	21.1	20.8	20.9	21.1	21.3
A. pullicarnis S23^T	21.2	ID	22.0	22.7	21.0	22.1	22.8	22.7	24.9	21.7	22.2	22.5	21.0	22.0	21.8	22.6	21.7	23.0	22.0	24.1	22.7
A. larvae BRTC-1^T	22.0	22.0	ID	22.2	20.8	20.9	22.1	21.8	21.8	21.6	22.0	21.9	21.1	22.0	21.9	21.4	20.8	21.3	21.1	21.7	21.5
A. gerneri MTCC 9824^T	21.9	22.7	22.2	ID	21.6	22.2	23.1	23.1	22.9	22.2	22.3	22.7	21.5	22.1	22.3	23.0	22.8	23.1	21.9	23.1	22.6
A. silvestris ANC 4999^T	20.9	21.0	20.8	21.6	ID	21.5	21.6	22.0	22.0	22.1	22.1	22.0	21.5	21.7	21.7	21.2	21.0	21.0	20.7	20.3	20.8
A. sichuanensis WCHAc060041^T	21.3	22.1	20.9	22.2	21.5	ID	27.0	24.2	27.1	22.9	23.1	26.6	22.5	22.0	22.1	23.2	22.5	22.0	21.4	21.6	23.2
A. defluvii WCHA30^T	21.4	22.8	22.1	23.1	21.6	27.0	ID	25.4	28.0	23.2	23.4	28.4	22.7	22.4	22.7	23.7	22.4	22.3	22.0	22.4	24.7
A. wuhouensis WCHA60^T	21.7	22.7	21.8	23.1	22.0	24.2	25.4	ID	24.3	24.2	24.5	24.4	23.3	22.1	22.7	24.6	22.9	22.0	22.3	22.6	27.5
A. rongchengensis WCHAc060115^T	21.0	24.9	21.8	22.9	22.0	27.1	28.0	24.3	ID	36.4	24.5	27.1	23.2	21.8	21.9	22.5	21.8	23.2	21.7	22.4	22.9
A. piscicola LW15^T	21.3	21.7	21.6	22.2	22.1	22.9	23.2	24.2	36.4	ID	25.2	24.2	23.6	21.3	22.3	22.0	21.6	21.8	21.3	21.3	22.2
A. guillouiae DSM 590^T	21.5	22.2	22.0	22.3	22.1	23.1	23.4	24.5	24.5	25.2	ID	26.2	25.1	22.0	22.4	22.2	21.9	22.4	21.9	22.9	22.1
A. bereziniae LMG 1003^T	21.7	22.5	21.9	22.7	22.0	26.6	28.4	24.4	27.1	24.2	26.2	ID	39.6	22.0	22.4	22.4	21.5	21.6	21.8	22.9	23.0
A. nematophilus sp. nov. A-IN1^T	20.8	21.0	21.1	21.5	21.5	22.5	22.7	23.3	23.2	23.6	25.1	39.6	ID	21.2	21.6	21.3	20.9	20.7	20.8	20.8	21.6
A. lanii 185^T	21.4	22.0	22.0	22.1	21.7	22.0	22.4	22.1	21.8	21.3	22.0	22.0	21.2	ID	22.5	22.9	22.2	21.8	21.7	22.4	21.7
A. equi 114^T	21.5	21.8	21.9	22.3	21.7	22.1	22.7	22.7	21.9	22.3	22.4	22.4	21.6	22.5	ID	22.6	22.5	22.0	21.6	21.5	21.8
A. cumulans WCHAc060092^T	21.3	22.6	21.4	23.0	21.2	23.2	23.7	24.6	22.5	22.0	22.2	22.4	21.3	22.9	22.6	ID	33.8	21.6	22.3	22.4	23.5
A. chengduensis WCHAc060005^T	21.1	21.7	20.8	22.8	21.0	22.5	22.4	22.9	21.8	21.6	21.9	21.5	20.9	22.2	22.5	33.8	ID	21.2	21.3	21.9	22.2
A. tandoii DSM 14970^T	20.8	23.0	21.3	23.1	21.0	22.0	22.3	22.0	23.2	21.8	22.4	21.6	20.7	21.8	22.0	21.6	21.2	ID	22.4	22.5	20.6
A. johnsonii DSM 69633^T	20.9	22.0	21.1	21.9	20.7	21.4	22.0	22.3	21.7	21.3	21.9	21.8	20.8	21.7	21.6	22.3	21.3	22.4	ID	22.0	21.1
A. variabilis NIPH 2171^T	21.1	24.1	21.7	23.1	20.3	21.6	22.4	22.6	22.4	21.3	22.9	22.9	20.8	22.4	21.5	22.4	21.9	22.5	22.0	ID	22.2
A. chinensis WCHAc010005^T	21.3	22.7	21.5	22.6	20.8	23.2	24.7	27.5	22.9	22.2	22.1	23.0	21.6	21.7	21.8	23.5	22.2	20.6	21.1	22.2	ID

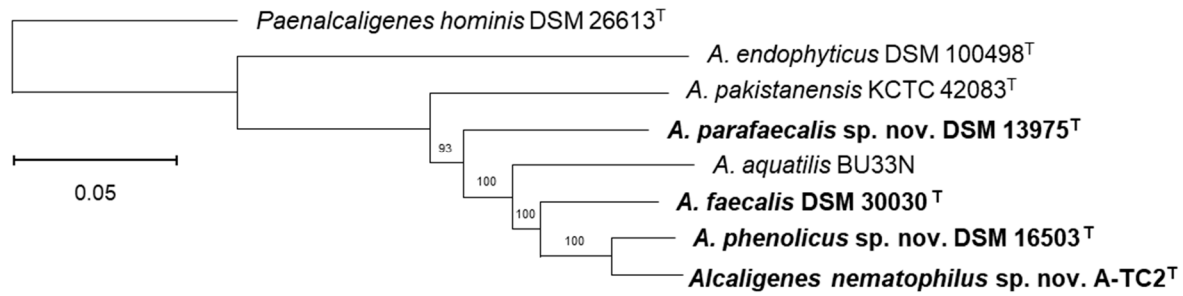

Figure 2. Phylogeny based on core genome sequences of all the species of the genus *Alcaligenes*. 408607 nucleotide positions (399 core genes) were used in the analyses. Numbers at the nodes represent SH-like branch supports. Phylogenomic trees were built using FastTree 2.1.10 based on the Generalized Time Reversible Model (GTR) [61]. Accession numbers of the sequences used in the analyses are shown in Table S1. Bold indicates novel taxonomic proposals.

Table 2. Pairwise comparison of digital DNA-DNA Hybridization (dDDH) scores (%) of all the species of the genus *Alcaligenes*. Accession numbers of the sequences used in the analyses are shown in Table S1. Colors indicate the degree of relatedness between bacterial species pairs.

	A. endophyticus DSM 100498^T	*A. pakistanensis* KCTC 42083^T	*A. parafaecalis* sp. nov. DSM 13975^T	*A. aquatilis* BU33N	*A. faecalis* DSM 30030^T	*A. phenolicus* sp. nov. DSM 16503^T	*A. nematophilus* sp. nov. A-TC9^T
A. endophyticus DSM 100498^T	ID	18.2	18.1	18.2	18.0	18.0	18.2
A. pakistanensis KCTC 42083^T	18.2	ID	32.7	29.5	30.8	30.5	30.4
A. parafaecalis sp. nov. DSM 13975^T	18.1	32.7	ID	34.1	36.8	35.7	35.5
A. aquatilis BU33N	18.2	29.5	34.1	ID	41.6	39.0	38.4
A. faecalis DSM 30030^T	18.0	30.8	36.8	41.6	ID	49.1	47.0
A. phenolicus sp. nov. DSM 16503^T	18.0	30.5	35.7	39.0	49.1	ID	66.3
A. nematophilus sp. nov. A-TC9^T	18.2	30.4	35.5	38.4	47.0	66.3	ID

Phylogenetic reconstructions based on 16S rRNA gene sequences show that E-TC7^T is more closely related to *Enterobacter bugandensis* EB-247^T (Figure S3A). The 16S rRNA gene sequence similarity score between E-TC7^T and this strain is 99.5% (Figure S3B). Based on phylogenies reconstructed from core-genome and core-proteomes, E-TC7^T is more closely related to *E. bugandensis* EB-247^T (Figures 3 and S5C). Similar phylogenies were reconstructed in previous studies [34,36]. The digital DNA-DNA hybridization (dDDH) score between E-TC7^T and this strain is 63.7% (Table 3). These values are below the 70% divergence threshold for prokaryotic species delineation [70,72,76].

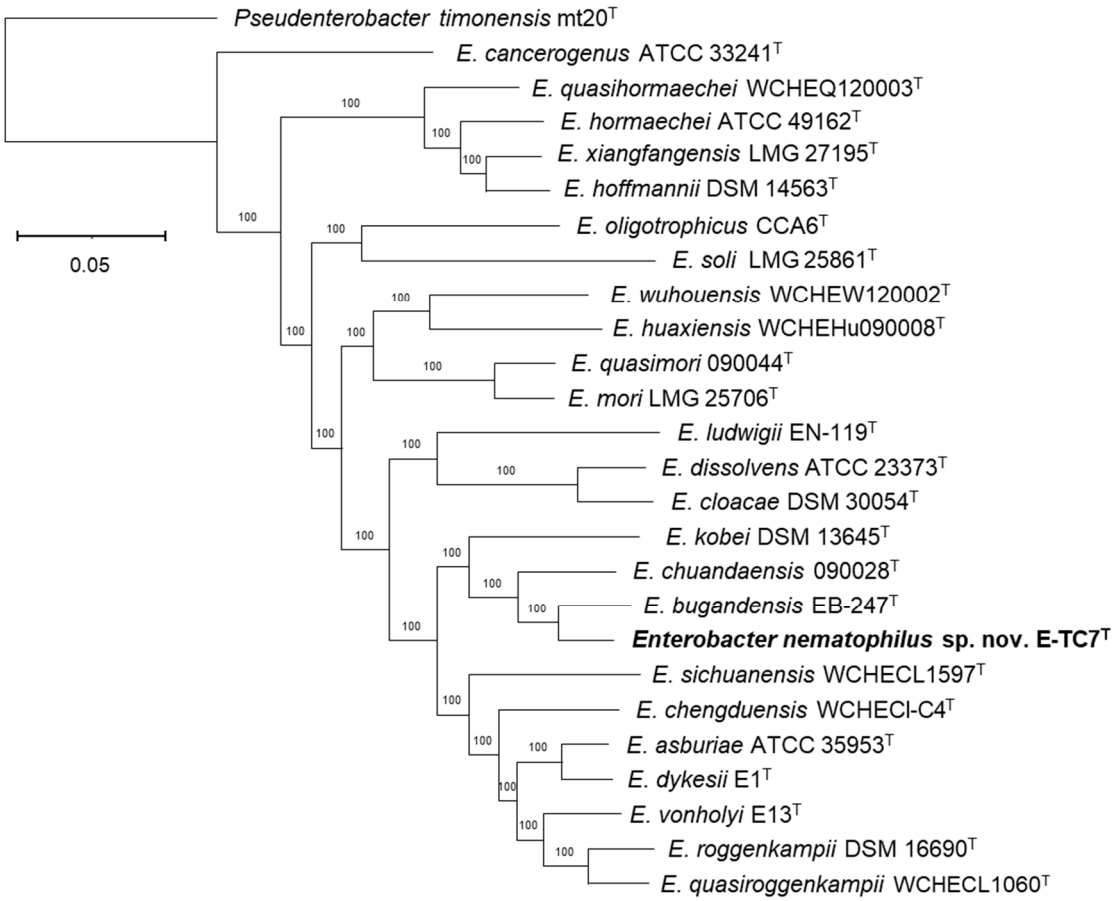

Figure 3. Phylogeny based on core genome sequences of all the species of the genus *Enterobacter*. 3055395 nucleotide positions (3071 core genes) were used in the analyses. Numbers at the nodes represent SH-like branch supports. Phylogenomic trees were built using FastTree 2.1.10 based on the Generalized Time Reversible Model (GTR) [61]. Accession numbers of the sequences used in the analyses are shown in Table S1. Bold indicates a novel taxonomic proposal.

Phylogenetic reconstructions based on 16S rRNA gene sequences show that K-TC2^T is more closely related to *Kaistia defluvii* JCM 18034^T (Figure S4A). The 16S rRNA gene sequence similarity score between K-TC2^T and this latest strain is 99.3% (Figure S4B). Similar phylogenies were reconstructed in previous studies [38,77]. Based on phylogenies reconstructed from core-genome and core-proteomes, K-TC2^T is more closely related to *K. defluvii* JCM 18034^T (Figures 4 and S5D). Recent studies have not reconstructed phylogenies using core genome sequences to compare [77]. The digital DNA-DNA hybridization (dDDH) score between K-TC2^T and this strain is 30.7% (Table 4). These values are below the 70% divergence threshold for prokaryotic species delineation [70,72,76].

Table 3. Pairwise comparison of digital DNA-DNA Hybridization (dDDH) scores (%) of all the species of the genus *Enterobacter*. Accession numbers of the sequences used in the analyses are shown in Table S1. Colors indicate the degree of relatedness between bacterial species pairs.

	E. cancerogenus ATCC33241^T	*E. quasihormaechei* WCHEQ120003^T	*E. hormaechei* ATCC 49162^T	*E. xiangfangensis* LMG27195^T	*E. hoffmannii* DSM 14563^T	*E. oligotrophicus* CCA6^T	*E. soli* LMG 25861^T	*E. wuhouensis* WCHEW120002^T	*E. huaxiensis* WCHEHu090008^T	*E. quasimori* 090044^T	*E. mori* LMG 25706^T	*E. ludwigii* EN-119^T	*E. dissolvens* ATCC 23373^T	*E. cloacae* DSM 30054^T	*E. kobei* DSM 13645^T	*E. chuandaensis* 090028^T	*E. bugandensis* EB-247^T	*E. nematophilus* sp. nov. E-TC7^T	*E. sichuanensis* WCHECL1597^T	*E. chengduensis* WCHECl-C4^T	*E. asburiae* ATCC 35953^T	*E. dykesii* E1^T	*E. vonholyi* E13^T	*E. roggenkampii* DSM 16690^T	*E. quasiroggenkampii* WCHECL1060^T
E. cancerogenus ATCC33241^T	ID	31.7	31.6	31.5	31.5	32.1	29.5	32.0	32.1	32.3	31.9	30.4	30.7	30.8	31.2	31.7	31.8	31.8	31.2	32.0	32.4	31.8	31.5	32.0	31.5
E. quasihormaechei WCHEQ120003^T	31.7	ID	51.6	52.8	53.5	33.5	29.8	33.9	33.7	34.9	34.0	31.4	32.1	32.3	33.4	35.3	36.7	35.3	32.4	33.9	34.2	33.7	33.3	34.3	33.6
E. hormaechei ATCC 49162^T	31.6	51.6	ID	60.0	58.0	33.8	30.2	33.9	33.8	35.0	34.2	31.6	32.4	32.9	33.7	35.4	35.7	35.3	32.6	34.5	34.6	33.8	33.3	34.3	33.7
E. xiangfangensis LMG27195^T	31.5	52.8	60.0	ID	66.6	33.8	30.2	33.8	33.8	35.0	34.2	31.5	32.5	32.6	33.4	35.2	35.7	35.2	32.8	34.1	34.8	33.9	33.7	34.7	34.0
E. hoffmannii DSM 14563^T	31.5	53.5	58.0	66.6	ID	33.8	30.0	33.7	33.8	34.8	34.1	31.4	32.1	32.5	33.4	35.0	35.5	34.9	32.5	34.0	34.4	33.5	33.1	34.2	33.5
E. oligotrophicus CCA6^T	32.1	33.5	33.8	33.8	33.8	ID	31.6	34.0	34.5	34.9	34.7	32.7	33.3	33.2	33.3	34.1	34.1	33.9	32.9	33.7	34.8	33.9	33.7	34.4	33.9
E. soli LMG 25861^T	29.5	29.8	30.2	30.2	30.0	31.6	ID	30.7	30.8	31.0	30.8	30.3	30.4	30.3	30.2	30.6	30.5	30.7	30.3	30.7	31.3	31.0	30.5	30.8	30.8
E. wuhouensis WCHEW120002^T	32.0	33.9	33.9	33.8	33.7	34.0	30.7	ID	39.6	38.0	37.9	32.8	33.3	33.2	33.9	36.2	35.8	36.3	34.1	35.9	37.7	36.6	35.6	36.0	35.6
E. huaxiensis WCHEHu090008^T	32.1	33.7	33.8	33.8	33.8	34.5	30.8	39.6	ID	37.6	37.4	32.1	32.8	32.7	33.5	35.2	35.0	35.1	33.6	35.2	36.4	35.3	34.5	35.1	34.6
E. quasimori 090044^T	32.3	34.9	35.0	35.0	34.8	34.9	31.0	38.0	37.6	ID	66.8	33.0	34.6	34.4	36.1	38.5	38.1	38.5	36.4	38.9	40.9	40.0	39.3	39.8	40.2
E. mori LMG 25706^T	31.9	34.0	34.2	34.2	34.1	34.7	30.8	37.9	37.4	66.8	ID	32.6	34.0	34.0	35.4	37.7	37.0	37.5	35.2	37.3	39.9	38.9	37.6	37.5	37.3
E. ludwigii EN-119^T	30.4	31.4	31.6	31.5	31.4	32.7	30.3	32.8	32.1	33.0	32.6	ID	34.4	34.2	34.6	34.7	34.8	34.7	34.6	35.0	36.1	35.5	35.0	35.5	34.9
E. dissolvens ATCC 23373^T	30.7	32.1	32.4	32.5	32.1	33.3	30.4	33.3	32.8	34.6	34.0	34.4	ID	62.1	34.9	35.6	35.5	35.8	37.1	35.5	36.7	36.1	35.6	36.1	36.0
E. cloacae DSM 30054^T	30.8	32.3	32.9	32.6	32.5	33.2	30.3	33.2	32.7	34.4	34.0	34.2	62.1	ID	35.7	35.6	35.6	35.5	36.9	36.2	37.2	35.8	35.5	36.3	35.8
E. kobei DSM 13645^T	31.2	33.4	33.7	33.4	33.4	33.3	30.2	33.9	33.5	36.1	35.4	34.6	34.9	35.7	ID	42.4	43.1	43.5	39.2	43.3	42.7	41.5	40.9	41.3	40.6
E. chuandaensis 090028^T	31.7	35.3	35.4	35.2	35.0	34.1	30.6	36.2	35.2	38.5	37.7	34.7	35.6	35.6	42.4	ID	53.9	56.1	39.7	42.7	45.6	44.5	43.1	43.4	42.7
E. bugandensis EB-247^T	31.8	36.7	35.7	35.7	35.5	34.1	30.5	35.8	35.0	38.1	37.0	34.8	35.5	35.6	43.1	53.9	ID	63.7	39.9	42.8	45.1	44.1	43.3	44.2	43.2
E. nematophilus sp. nov. E-TC7^T	31.8	35.3	35.3	35.2	34.9	33.9	30.7	36.3	35.1	38.5	37.5	34.7	35.8	35.5	43.5	56.1	63.7	ID	40.2	42.9	45.7	44.9	43.6	43.8	42.7
E. sichuanensis WCHECL1597^T	31.2	32.4	32.6	32.8	32.5	32.9	30.3	34.1	33.6	36.4	35.2	34.6	37.1	36.9	39.2	39.7	39.9	40.2	ID	42.6	45.2	44.2	44.2	45.5	44.6
E. chengduensis WCHECl-C4^T	32.0	33.9	34.5	34.1	34.0	33.7	30.7	35.9	35.2	38.9	37.3	35.0	35.5	36.2	43.3	42.7	42.8	42.9	42.6	ID	52.7	50.9	49.7	48.9	49.5
E. asburiae ATCC 35953^T	32.4	34.2	34.6	34.8	34.4	34.8	31.3	37.7	36.4	40.9	39.9	36.1	36.7	37.2	42.7	45.6	45.1	45.7	45.2	52.7	ID	69.3	57.2	51.7	51.7
E. dykesii E1^T	31.8	33.7	33.8	33.9	33.5	33.9	31.0	36.6	35.3	40.0	38.9	35.5	36.1	35.8	41.5	44.5	44.1	44.9	44.2	50.9	69.3	ID	57.4	51.1	51.5
E. vonholyi E13^T	31.5	33.3	33.3	33.7	33.1	33.7	30.5	35.6	34.5	39.3	37.6	35.0	35.6	35.5	40.9	43.1	43.3	43.6	44.2	49.7	57.2	57.4	ID	56.0	56.4
E. roggenkampii DSM 16690^T	32.0	34.3	34.3	34.7	34.2	34.4	30.8	36.0	35.1	39.8	37.5	35.5	36.1	36.3	41.3	43.4	44.2	43.8	45.5	48.9	51.7	51.1	56.0	ID	65.1
E. quasiroggenkampii WCHECL1060^T	31.5	33.6	33.7	34.0	33.5	33.9	30.8	35.6	34.6	40.2	37.3	34.9	36.0	35.8	40.6	42.7	43.2	42.7	44.6	49.5	51.7	51.5	56.4	65.1	ID

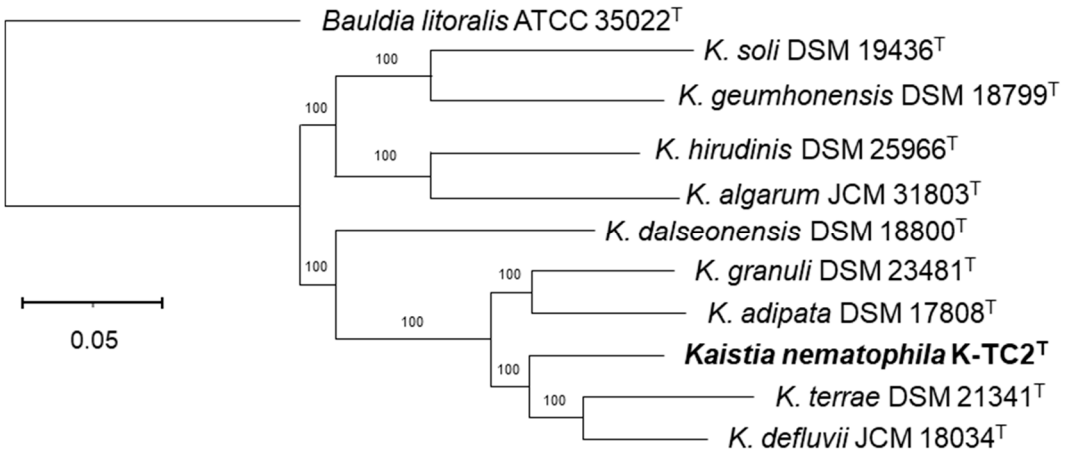

Figure 4. Phylogeny based on core genome sequences of all the species of the genus *Kaistia.* 543369 nucleotide positions (508 core genes) were used in the analyses. Numbers at the nodes represent SH-like branch supports. Phylogenomic trees were built using FastTree 2.1.10 based on the Generalized Time Reversible Model (GTR) [61]. Accession numbers of the sequences used in the analyses are shown in Table S1. Bold indicates a novel taxonomic proposal.

Table 4. Pairwise comparison of digital DNA-DNA Hybridization (dDDH) scores (%) of all the species of the genus *Kaistia*. Accession numbers of the sequences used in the analyses are shown in Table S1. Colors indicate the degree of relatedness between bacterial species.

	K. soli DSM 19436^T	*K. geumhonensis* DSM 18799^T	*K. hirudinis* DSM 25966^T	*K. algarum* JCM 31803^T	*K. dalseonensis* DSM 18800^T	*K. granuli* DSM 23481^T	*K. adipata* DSM 17808^T	*K. nematophila* sp. nov. K-TC2^T	*K. terrae* DSM 21341^T	*K. defluvii* JCM 18034^T
K. soli DSM 19436^T	ID	22.2	21.0	21.0	21.3	20.8	20.9	21.2	20.7	21.0
K. geumhonensis DSM 18799^T	22.2	ID	21.5	20.8	21.3	21.0	21.3	21.5	20.7	21.3
K. hirudinis DSM 25966^T	21.0	21.5	ID	24.1	21.8	21.2	21.4	21.5	20.8	21.4
K. algarum JCM 31803^T	21.0	20.8	24.1	ID	21.4	21.0	20.9	21.2	20.9	21.1
K. dalseonensis DSM 18800^T	21.3	21.3	21.8	21.4	ID	21.8	21.9	22.2	21.8	22.1
K. granuli DSM 23481^T	20.8	21.0	21.2	21.0	21.8	ID	30.0	27.8	27.1	27.4
K. adipata DSM 17808^T	20.9	21.3	21.4	20.9	21.9	30.0	ID	28.0	25.7	27.1
K. nematophila sp. nov. K-TC2^T	21.2	21.5	21.5	21.2	22.2	27.8	28.0	ID	29.2	30.9
K. terrae DSM 21341^T	20.7	20.7	20.8	20.9	21.8	27.1	25.7	29.2	ID	30.7
K. defluvii JCM 18034^T	21.0	21.3	21.4	21.1	22.1	27.4	27.1	30.9	30.7	ID

Based on these genomic divergence values, we propose the creation of the following new taxa: *Acinetobacter nematophilus* sp. nov. with A-IN1^T (=CCM 9231^T =CCOS 2018^T) as the type strain, *Alcaligenes nematophilus* sp. nov. with A-TC2^T (=CCM 9230^T =CCOS 2017^T) as the type strain, *Enterobacter nematophilus* sp. nov. with E-TC7^T (=CCM 9232^T =CCOS 2020^T) as the type strain, and *Kaistia nematophila* sp. nov. with K-TC2^T (=CCM 9239^T =CCOS 2022^T) as the type strain. In addition, we propose the elevation of *Alcaligenes faecalis* subsp. *faecalis*, *Alcaligenes faecalis* subsp. *phenolicus*, and *Alcaligenes faecalis* subsp. *parafaecalis* to the

species level and therefore we propose the creation of *Alcaligenes parafaecalis* sp. nov. with DSM 13975^T as the type strain, and *Alcaligenes phenolicus* sp. nov. with DSM 16503^T as the type strain.

3.2. Genomic Features

The genomes of thirteen type strains of the genera *Acinetobacter, Alcaligenes*, *Enterobacter*, and *Kaistia* were sequenced in this study. Their main characteristics are summarized in Tables S2–S4. The main characteristics of the genomes of the novel species are as follows. The genome of *Acinetobacter nematophilus* A-IN1^T contains 4360075 bp, a G+C content of 38.49, and 4046 proteins. The genome of *Alcaligenes nematophilus* sp. nov. A-TC2^T contains 4251628 bp, a G+C content of 56.41, and 3892 proteins. The genome of *Enterobacter nematophilus* sp. nov. E-TC7^T contains 4708215bp, a G+C content of 56.36, and 4289 proteins. The genome of *Kaistia nematophila* sp. nov. K-TC2^T contains 5165915 bp, a G+C content of 66.75, and 4789 proteins (Tables S2 and S3). These genomes are predicted to be more than 99% complete and contain less than 2% contamination (Table S4).

3.3. Physiological and Biochemical Characteristics

Biochemical tests show that *Acinetobacter nematophilus* A-IN1^T, *Alcaligenes nematophilus* A-TC2^T, *Enterobacter nematophilus* E-TC7^T, and *Kaistia nematophila* K-TC2^T exhibit biochemical capacities that are similar to the biochemical capacities of several members of their respective genus (Table 5). However, these strains also exhibit unique biochemical capacities that differ from the biochemical capacities of their most closely related taxa (Table 5).

In particular, *Acinetobacter nematophilus* A-IN1^T does not hydrolyze arginine, unlike *Acinetobacter bereziniae* DSM 25435^T, its most closely related taxon. *Acinetobacter bereziniae* DSM 25435^T has been biochemically characterized previously using different biochemical tests than the tests used in this study. However, we observed that *Acinetobacter bereziniae* DSM 25435^T utilizes citrate, which is in good agreement with that previous study [78].

Alcaligenes nematophilus A-TC2^T is negative for β-galactosidase, tryptophan deaminase, and gelatinase, unlike *Alcaligenes faecalis subsp. phenolicus* DSM 16503^T (proposed name: *Alcaligenes phenolicus*), its most closely related taxon. In addition, *Alcaligenes nematophilus* A-TC2^T does not produce hydrogen sulfide or indole, unlike *Alcaligenes faecalis subsp. phenolicus* DSM 16503^T, which produces these molecules. Lastly, *Alcaligenes nematophilus* A-TC2^T does not oxidize mannitol, inositol, rhamnose, or amygdalin, unlike *Alcaligenes faecalis subsp. phenolicus* DSM 16503^T which oxidizes these compounds. In previous studies, *Alcaligenes faecalis subsp. phenolicus* DSM 16503^T was also reported to hydrolase gelatin, while *Alcaligenes endophyticus* DSM 100498^T, *Alcaligenes faecalis subsp. faecalis* DSM 30030^T (Proposed name: *Alcaligenes faecalis*), and *Alcaligenes faecalis subsp. parafaecalis* DSM 13975^T (Proposed name: *Alcaligenes parafaecalis*) were reported as gelatinase negative [26,28]. Our results are therefore in good agreement with these previous studies [26,28].

Enterobacter nematophilus E-TC7^T oxidizes sucrose and melibiose, unlike *Enterobacter bugandensis* STN0717-56^T, its most closely related taxon. In previous studies, it has been reported that most *Enterobacter* species do not produce indole or sulfides, but produce acetoin, and are mostly positive for citrate utilization. Our results are in good agreement with these studies [32,34,36].

Kaistia nematophila K-TC2^T is positive for β-galactosidase, arginine dihydrolase, ornithine decarboxylase, and citrate utilization, unlike *Kaistia defluvii* JCM 18034^T, its most closely related taxon. Moreover, *Kaistia nematophila* K-TC2^T produces acetoin, unlike *Kaistia defluvii* JCM 18034^T. In addition, *Kaistia nematophila* K-TC2^T reduces nitrogen dioxide and oxidizes rhamnose and arabinose, unlike *Kaistia defluvii* JCM 18034^T (Table 1). We also observe that most *Kaistia* species are gelatinase negative, as has been also observed in previous studies [38,39].

Table 5. Phenotypic characters of the different strains described in this study and of the type strains of closely related species. 1: *Acinetobacter bereziniae* DSM 25435^T; 2: *Acinetobacter guillouiae* DSM 590^T; 3: *Acinetobacter nematophilus* sp. nov. A-IN1^T; 4: *Alcaligenes endophyticus* DSM 100498^T; 5: *Alcaligenes faecalis* subsp. *faecalis* DSM 30030^T (Proposed name: *Alcaligenes faecalis*); 6: *Alcaligenes nematophilus* sp. nov. A-TC2^T; 7: *Alcaligenes faecalis* subsp. *parafaecalis* DSM 13975^T (Proposed name: *Alcaligenes parafaecalis* sp. nov.); 8: *Alcaligenes faecalis* subsp. *phenolicus* DSM 16503^T (Proposed name: *Alcaligenes phenolicus* sp. nov.); 9: *Enterobacter bugandensis* STN0717-56^T; 10: *Enterobacter chuandaensis* 090028^T; 11: *Enterobacter kobei* DSM 13645^T; 12: *Enterobacter nematophilus* sp. nov. E-TC7^T; 13: *Kaistia algarum* JCM 31803^T; 14: *Kaistia dalseonensis* DSM 18800^T; 15: *Kaistia defluvii* JCM 18034^T; 16: *Kaistia geumhonensis* DSM 18799^T; 17: *Kaistia nematophila* sp. nov. K-TC2^T; and 18: *Kaistia terrae* DSM 21341^T. +: positive reaction. −: negative reaction.

	Bacterial Strain																	
	Acinetobacter			***Alcaligenes***					***Enterobacter***					***Kaistia***				
Biochemical test	1	2	3	4	5	6	7	8	9	10	11	12	13	14	15	16	17	18
β-Galactosidase	−	−	−	−	−	−	−	+	+	+	+	+	+	+	−	+	+	+
Arginine dihydrolase	+	+	−	+	+	+	+	+	+	+	+	+	−	+	−	+	+	−
Lysine decarboxylase	−	−	−	−	+	+	+	+	+	−	+	+	−	+	−	+	−	−
Ornithine decarboxylase	−	−	−	+	−	+	+	+	+	+	+	+	−	+	−	+	+	−
Citrate utilization	+	+	+	+	+	+	+	+	+	+	+	+	+	+	−	+	+	+
H_2S production	−	−	−	−	−	−	−	+	−	−	−	−	−	−	−	−	−	−
Urease	−	−	−	+	+	+	+	+	+	−	+	+	+	+	+	+	+	+
Tryptophan deaminase	−	−	−	−	+	−	−	+	−	−	−	−	−	−	−	−	−	−
Indole production	−	−	−	−	−	−	−	+	−	−	−	−	−	−	−	−	−	−
Acetoin production	+	+	+	+	+	+	+	+	+	+	+	+	−	+	+	−	−	−
Gelatinase	−	−	−	−	−	−	−	+	+	−	+	+	−	−	−	−	−	−
Glucose oxidation	+	−	+	−	−	−	−	−	+	+	+	+	−	−	−	−	−	−
Mannitol oxidation	−	−	−	−	−	−	−	+	+	+	+	+	−	−	−	−	−	−
Inositol oxidation	−	−	−	−	−	−	−	+	+	−	−	+	−	−	−	−	−	−
Sorbitol oxidation	−	−	−	−	−	−	−	−	+	−	+	+	−	−	−	−	−	−
Rhamnose oxidation	+	−	+	−	−	−	−	+	+	+	+	+	−	−	−	−	+	−
Sucrose oxidation	−	−	−	−	−	−	−	−	+	+	+	−	−	−	−	−	−	−

Table 5. *Cont.*

	Bacterial Strain																	
	Acinetobacter			***Alcaligenes***				***Enterobacter***						***Kaistia***				
Melibiose oxidation	+	−	+	−	−	−	−	−	+	−	+	−	−	−	−	−	−	−
Amygdalin oxidation	−	−	−	−	−	−	−	+	+	+	+	+	−	−	−	−	−	−
Arabinose oxidation	+	−	+	−	−	−	−	−	+	+	+	+	−	−	−	−	+	−
(Cytochrome) oxidase	−	−	−	+	+	+	+	+	+	+	+	+	+	+	+	+	+	+
Catalase	+	+	+	+	+	+	+	+	+	+	+	+	+	+	+	+	+	+
NO_2 production	−	−	−	−	−	−	−	−	−	−	+	−	−	+	−	−	−	−
NO_2 reduction to N_2 gas	−	−	−	−	−	−	−	+	+	+	−	+	−	−	−	+	+	−

Noteworthily, we observed that the biochemical capacities of the newly isolated bacteria are, in some cases, very similar to the biochemical capacities of their most closely related species. For instance, *Acinetobacter nematophilus* A-IN1^T and *Acinetobacter bereziniae* DSM 25435^T differ only in their capacity to digest arginine, and *Enterobacter nematophilus* E-TC7^T and *Enterobacter bugandensis* STN0717-56^T differ only in their capacity to oxidize sucrose and melibiose (Table 5). In other cases, however, closely related species show greater phenotypic divergencies. For instance, *Alcaligenes nematophilus* A-TC2^T and *Alcaligenes faecalis subsp. phenolicus* DSM 16503^T differ in several traits, in a similar manner as *Kaistia nematophila* K-TC2^T, *Kaistia defluvii* JCM 18034^T, and *Kaistia terrae* DSM 21341^T do. Such divergencies might reflect adaptations to their local environments and could potentially impact the outcome of interspecific interactions.

3.4. Ecology

The ecology of the type strains of the novel species described in this study and their nematode hosts have been studied previously [13–15]. An interesting aspect of these bacterial strains is that all of them were isolated from soil-borne nematodes. In one of our previous studies, we evaluated the insect-killing abilities of one of them, *Oscheius tipulae* TC2, the host of *A. nematophilus* A-TC2^T and *K. nematophila* K-TC2^T [13]. We observed that this nematode isolate was highly lethal against the mediterranean fly and it rapidly and effectively killed its eggs, larvae, and pupae, and also interferes with insect metamorphosis [13]. We did not extensively test the insect-killing abilities of the other two nematodes that host the other bacterial strains described in this study, *Acrobeloides bodenheimeri* TC7 and IN1 (unidentified), but they are also able to kill insects as we recovered them from soil samples using *C. capitata* pupae and *G. mellonella* larvae as baits, respectively [13–15]. In an additional study, we tested the contribution of the bacterial strains isolated in this study to the insect-killing abilities of their nematode hosts [14]. By injecting the bacteria directly in the hemocoels of *G. mellonella* larvae, we observed that they all were highly pathogenic. These bacterial strains therefore might be promising biocontrol agents. Further studies are required to untap their real potential under agriculturally relevant settings.

3.5. Conclusions

Considering the biochemical and genomic differences of the strains analyzed in this study, we propose the following new species: *Acinetobacter nematophilus* sp. nov. with A-IN1^T (=CCM 9231^T =CCOS 2018^T) as the type strain, *Alcaligenes nematophilus* sp. nov. with A-TC2^T (=CCM 9230^T =CCOS 2017^T) as the type strain, *Enterobacter nematophilus* sp. nov. with E-TC7^T (=CCM 9232^T =CCOS 2020^T) as the type strain, and *Kaistia nematophila* sp. nov. with K-TC2^T (=CCM 9239^T =CCOS 2022^T) as the type strain. In addition, we propose the elevation of *Alcaligenes faecalis* subsp. *faecalis*, *Alcaligenes faecalis* subsp. *parafaecalis*, and *Alcaligenes faecalis* subsp. *phenolicus* to the species level. Therefore, we propose the creation of *Alcaligenes parafaecalis* sp. nov. with DSM 13975^T as the type strain, and *Alcaligenes phenolicus* sp. nov. with DSM 16503^T as the type strain.

3.6. Protologues

Emended description of *Alcaligenes faecalis*

(fae.ca'lis. L. fem. n. *faex* (gen. *faecis*), dregs, feces; L. masc./fem. adj. suff. *-alis*, suffix denoting pertaining to; N.L. masc./fem. adj. *faecalis*, pertaining to feces, fecal). This amended description results from the proposal to elevate *Alcaligenes faecalis* subsp. *faecalis* to the species level. The description is the same as given for *Alcaligenes faecalis* by Castellani and Chalmers (1919), updated by Kersters and De Ley (1984) and amended by Schroll et al. (2001) and Rehfuss and Urban (2005) [23,25,28,79] with the following additions. The genome of the type strain, DSM 30030^T, contains 4003996 base pairs, 3706 proteins, and a G+C content of 56.65%. The genome and the 16S rRNA gene sequences of DSM 30030^T were deposited in the NCBI under the accession numbers JAPKNC01 and OP804215, respectively. The type strain is ATCC 8750^T (=DSM 30030^T =ATCC 8750^T =CCUG 1814^T =CIP 55.84^T

=CIP 60.80^T, HAMBI 1907^T =IFO 13111^T =JCM 1474^T =JCM 20522^T =JCM 20663^T =LMG 1229^T =NBRC 13111^T =NCAIM B.01104^T =NCIB 8156^T =NCIMB 8156^T =NCTC 11953^T =VKM B-1518^T).

Description of *Acinetobacter nematophilus* sp. nov.

(ne.ma.to'phi.lus. N.L. masc. adj. suff. *-philus*, loving or having affinity for; N.L. masc. adj. *nematophilus*, nematode-loving). Cells are short rods, approx. 0.9–1.3 µm wide and 1.2–1.4 µm long (Figure S6A). Growth is observed between 20–32 °C. Poor growth occurs at 37 °C. The optimal temperature for growth is 30 °C. Bacterial growth occurs at pH between 5–9 (optimum 5–7) and not at pH 3. Bacterial growth occurs in LB medium containing between 1–3% NaCl (optimum 1–2%). Bacterial growth is inhibited in LB containing more than 3% NaCl. It is negative for β-galactosidase, arginine dihydrolase, lysine and ornithine decarboxylases, urease, tryptophan deaminase, and cytochrome oxidase. It does not produce hydrogen sulfide, indole, or nitrites. It does not digest gelatin. It does not oxidize mannitol, inositol, sorbitol, sucrose, or amygdalin. It does not reduce nitrites. It is positive for catalase, utilizes citrate, produces acetoin, and oxidizes glucose, rhamnose, melibiose, and arabinose. The genome and the 16S rRNA gene sequences of the type strain, A-IN1^T, were deposited in the NCBI databank under the accession numbers JAPKMY01 and OP818110, respectively. The genome assembled contains 4360075 base pairs, 4046 proteins, and a G+C content of 38.49%. The type strain of the species is A-IN1^T (=CCM 9231^T =CCOS 2018^T). A-IN1^T was isolated from an unidentified soil-borne nematode, IN1, collected in Tunis (Tunisia).

Description of *Alcaligenes nematophilus* sp. nov.

(ne.ma.to'phi.lus. N.L. masc. adj. suff. *-philus*, loving or having affinity for; N.L. masc. adj. *nematophilus*, nematode-loving). Cells are rod-shaped, approx. 0.5–0.8 µm wide and 1.3–1.9 µm long (Figure S6B). Growth is observed between 20–42 °C. The optimal temperature for growth is 30 °C. Bacterial growth occurs at pH between 7–9 (optimum 7–8) and not at pH below 5. Bacterial growth occurs in LB medium containing between 1–7% NaCl (optimum 1–3%). It is Negative for β-galactosidase and tryptophan deaminase. It does not produce hydrogen sulfide, indole, or nitrites. It does not digest gelatin. It does not oxidase mannitol, inositol, sorbitol, sucrose, amygdalin, glucose, rhamnose, melibiose, or arabinose. It does not reduce nitrites. It is positive for arginine dihydrolase, lysine and ornithine decarboxylases, urease, cytochrome oxidase, and catalase. It utilizes citrate and produces acetoin. The genome and the 16S rRNA gene sequences of the type strain, A-TC2^T, were deposited in the NCBI databank under the accession numbers JAPKMZ01 and OP804216, respectively. The genome assembled contains 4251628 base pairs, 3892 proteins, and a G+C content of 56.41%. The type strain of the species is A-TC2^T (=CCM 9230^T =CCOS 2017^T). A-TC2^T was isolated from *Oscheius tipulae* TC2 nematodes collected in Takilsa (Tunisia).

Description of *Alcaligenes parafaecalis* sp. nov.

(para.fae.ca'lis. (Gr. prep. *para*, beside, alongside of, near, like; N.L. masc./fem. adj. *faecalis*, specific epithet; N.L. masc./fem. adj. *parafaecalis*, intended to mean alongside of the species *Alcaligenes faecalis*). *Alcaligenes parafaecalis* sp. nov. results from the proposal to elevate *Alcaligenes faecalis* subsp. *parafaecalis* to the species level. The description of *A. parafaecalis* sp. nov. is the same as given for *Alcaligenes faecalis* subsp. *parafaecalis* by [25]. However, we found that it does not digest gelatin at 30 °C. The genome and the 16S rRNA gene sequences of the type strain, DSM 13975^T, were deposited in the NCBI under the accession number JAPKNA01 and OP804213, respectively. The genome assembled contains 4004626 base pairs, 3624 proteins, and a G+C content of 56.02%. The type strain of the species is DSM 13975^T (=CIP 106866^T =CCUG 48316^T =G^T).

Description of *Alcaligenes phenolicus* sp. nov.

(phe.nol.i'cus. N. L. n. phenol common name for industrial solvent hydroxybenzene; N.L. masc. adj. *phenolicus* pertaining to phenol). *Alcaligenes phenolicus* sp. nov. results from the proposal to elevate *Alcaligenes faecalis* subsp. *phenolicus* to the species level. The description of *A. phenolicus* sp. nov. is the same as given for *Alcaligenes faecalis* subsp. *phenolicus* by Rehfuss and Urban (2005) [28]. The genome and the 16S rRNA gene sequences were deposited in the NCBI under the accession number JAPKNB01 and OP804214, respectively. The genome assembled contains 4238760 base pairs, 3909 proteins, and a G+C content of 56.42%. The type strain of the species is J^T (=DSM 16503^T =NRRL B-41076^T).

Description of *Enterobacter nematophilus* sp. nov.

(ne.ma.to'phi.lus. N.L. masc. adj. suff. *-philus*, loving or having affinity for; N.L. masc. adj. *nematophilus*, nematode-loving). Cells are rod-shaped, approx. 0.9–1.2µm wide and 2.0–2.5µm long (Figure S6C). Growth is observed between 20–42 °C. The optimal temperature for growth is 37 °C. Bacterial growth occurs at pH between 5–9 (optimum 5–7) and not at pH 3. Bacterial growth occurs in LB medium containing between 1–7% NaCl (optimum 1–5%). It is negative for tryptophan deaminase. It does not produce hydrogen sulfide, indole, or nitrites. It does not oxidase sucrose or melibiose. It is positive for β-galactosidase, digests gelatin, oxidizes mannitol, inositol, sorbitol, amygdalin, glucose, rhamnose, and arabinose. It is positive for arginine, lysine, and ornithine decarboxylases, urease, cytochrome oxidase, and catalase. It utilizes citrate, produces acetoin and reduces nitrites. The genome and the 16S rRNA gene sequences of the type strain, E-$TC7^T$, were deposited in the NCBI under the accession number JAPKNE01 and OP818089, respectively. The genome assembled contains 4708215 base pairs, 4289 proteins, and a G+C content of 56.36%. The type strain of the species is E-$TC7^T$ (=CCM 9232^T =CCOS 2020^T). E-$TC7^T$ was isolated from *Acrobeloides bodenheimeri* TC7 nematodes collected in Takilsa (Tunisia).

Description of *Kaistia nematophila* sp. nov.

(ne.ma.to'phi.la. N.L. n. *nematoda* nematode; N.L. fem. adj. suff. *-phila*, loving or having affinity for; N.L. fem. adj. *nematophila*, nematode-loving). Cells are short rods, approx. 0.8–1.2µm wide and 1.1–1.6 µm long (Figure S6D). Growth is observed between 20–35 °C. The optimal temperature for growth is 28–30 °C. Bacterial growth occurs at pH between 5–8 (optimum 5–7) and not at pH 3 or 9. Bacterial growth occurs in LB medium containing 1% NaCl. Bacterial growth is inhibited in LB containing more than 1% NaCl. It is negative for tryptophan deaminase and lysine decarboxylase. It does not produce hydrogen sulfide, indole, acetoin, or nitrites. It does not oxidase sucrose, melibiose, mannitol, inositol, sorbitol, amygdalin, or glucose. It does not digest gelatin. It reduces nitrites and oxidizes rhamnose and arabinose. It is positive for β-galactosidase, arginine dihydrolase, ornithine decarboxylase, urease, cytochrome oxidase, and catalase. It utilizes citrate. The genome and the 16S rRNA gene sequences of the type strain, K-$TC2^T$, were deposited in the NCBI under the accession numbers JAPKNK01 and OP804305, respectively. The genome assembled contains 5165915 base pairs, 4789 proteins, and a G+C content of 66.75%. The type strain of the species is K-$TC2^T$ (=CCM 9239^T =CCOS 2022^T). K-$TC2^T$ was isolated from *Oscheius tipulae* TC2 nematodes collected in Takilsa (Tunisia).

Supplementary Materials: The following supporting information can be downloaded at: https://www.mdpi.com/article/10.3390/taxonomy3010012/s1, Figure S1: Phylogenetic reconstruction based on 16S rRNA gene sequences of several *Acinetobacter* species with validly published names; Figure S2: Phylogenetic reconstruction based on 16S rRNA gene sequences of all *Alcaligenes* species with validly published names; Figure S3: Phylogenetic reconstruction based on 16S rRNA gene sequences of all *Enterobacter* species with validly published names; Figure S4: Phylogenetic reconstruction based on 16S rRNA gene sequences of all *Kastia* species with validly published names; Figure S5: Phylogenetic reconstructions based on core proteome sequences; Figure S6: Photographs of the newly described bacterial species; Table S1: National Center for Biotechnology Information (NCBI) accession numbers

of the bacterial sequences used in this study; Table S2: Features of the genomes generated in this study (Part 1); Table S3: Features of the bacterial genomes generated in this study (Part 2); Table S4: Completeness (%) and contamination (%) of the bacterial genomes generated in this study assessed by checkM; Table S5: Source of the bacterial strains used in this study.

Author Contributions: Conceptualization, R.A.R.M. and S.K.; Data curation, R.A.R.M.; Formal analysis, R.A.R.M.; Funding acquisition, R.A.R.M., M.F.B. and S.K. Investigation, R.A.R.M., A.L., A.H.B., M.M. and C.T. Methodology, R.A.R.M., A.L., A.H.B., M.M. and C.T.; Project administration, R.A.R.M., M.F.B. and S.K.; Resources, R.A.R.M., M.F.B. and S.K.; Supervision, R.A.R.M., M.F.B. and S.K.; Validation, R.A.R.M.; Visualization, R.A.R.M.; Writing—original draft, R.A.R.M.; Writing—review & editing, R.A.R.M., A.H.B., C.T. and S.K. All authors have read and agreed to the published version of the manuscript.

Funding: This study was financed the Swiss National Science Foundation (Grant 186094 to RARM) and partially financed by the federated research project "Gestion intégrée contre la Cératite pour la promotion d'une agriculture durable" (PRF2019-D6P2) of Ministry of Higher Education and Scientific Research, Tunisia. The work of AHB was supported by a Postdoctoral Swiss Government Excellence Scholarship (Grant Nr. 2021.0463 to AHB). The work of C.T. is supported by the Swiss National Science Foundation (Grant 180142 to Diego Gonzalez).

Data Availability Statement: All data are provided within the manuscript. Whole genome sequences of A-IN1^T, A-TC2^T, E-TC7^T, and K-TC2^T are deposited in the National Center for Biotechnology Information (NCBI) databank under the accession numbers JAPKMY01, JAPKMZ01, JAPKNE01, and JAPKNK01, respectively; and the 16S rRNA gene sequences under the accession numbers and OP818110, OP804216, OP818089, and OP804305, respectively.

Acknowledgments: We thank the Swiss National Science Foundation and the Institute of Biology of the University of Neuchâtel (Switzerland), the University of Carthage and the National Agronomic Institute of Tunisia for their support.

Conflicts of Interest: The authors declare no conflict of interest and that no humans or animals were used for experimental purposes.

References

1. Ogier, J.-C.; Frayssinet, M.; Gaudriault, S. Entomopathogenic nematode-associated microbiota: From monoxenic paradigm to pathobiome. *Microbiome* **2020**, *8*, 25. [CrossRef] [PubMed]
2. Shokoohi, E.; Mashela, P.W.; Machado, R.A.R. Bacterial communities associated with *Zeldia punctata*, a bacterivorous soil-borne nematode. *Int. Microbiol.* **2022**, *25*, 207–216. [CrossRef] [PubMed]
3. Hill, V.; Kuhnert, P.; Erb, M.; Machado, R.A.R. Identification of *Photorhabdus* symbionts by MALDI-TOF MS. *Microbiology* **2020**, *166*, 522–530. [CrossRef] [PubMed]
4. Machado, R.A.R.; Thönen, L.; Arce, C.; Theepan, V.; Prada, F.; Wüthrich, D.; Robert, C.A.M.; Vogiatzaki, E.; Shi, Y.-M.; Schaeren, O.P. Engineering bacterial symbionts of nematodes improves their biocontrol potential to counter the western corn rootworm. *Nat. Biotechnol.* **2020**, *38*, 600–608. [CrossRef]
5. Waterfield, N.R.; Ciche, T.; Clarke, D. *Photorhabdus* and a host of hosts. *Annu. Rev. Microbiol.* **2009**, *63*, 557–574. [CrossRef]
6. Zhou, X.; Kaya, H.K.; Heungens, K.; Goodrich-Blair, H. Response of ants to a deterrent factor (s) produced by the symbiotic bacteria of entomopathogenic nematodes. *Appl. Environ. Microbiol.* **2002**, *68*, 6202–6209. [CrossRef] [PubMed]
7. Murfin, K.E.; Dillman, A.R.; Foster, J.M.; Bulgheresi, S.; Slatko, B.E.; Sternberg, P.W.; Goodrich-Blair, H. Nematode-bacterium symbioses—Cooperation and conflict revealed in the "Omics" age. *Biol. Bull.* **2012**, *223*, 85–102. [CrossRef] [PubMed]
8. Rafaluk-Mohr, C.; Ashby, B.; Dahan, D.A.; King, K.C. Mutual fitness benefits arise during coevolution in a nematode-defensive microbe model. *Evol. Lett.* **2018**, *2*, 246–256. [CrossRef]
9. Jones, R.S.; Fenton, A.; Speed, M.P.; Mappes, J. Investment in multiple defences protects a nematode-bacterium symbiosis from predation. *Anim. Behav.* **2017**, *129*, 1–8. [CrossRef]
10. Hodgkin, J.; Kuwabara, P.E.; Corneliussen, B. A novel bacterial pathogen, *Microbacterium nematophilum*, induces morphological change in the nematode *C. elegans*. *Curr. Biol.* **2000**, *10*, 1615–1618. [CrossRef]
11. Emelianoff, V.; Chapuis, E.; Le Brun, N.; Chiral, M.; Moulia, C.; Ferdy, J.-B. A survival-reproduction trade-off in entomopathogenic nematodes mediated by their bacterial symbionts. *Evol. Int. J. Org. Evol.* **2008**, *62*, 932–942. [CrossRef] [PubMed]
12. Zhang, X.; Machado, R.A.R.; van Doan, C.; Arce, C.C.M.; Hu, L.; Robert, C.A.M. Entomopathogenic nematodes increase predation success by inducing cadaver volatiles that attract healthy herbivores. *Elife* **2019**, *8*, e46668. [CrossRef]
13. Loulou, A.; M'saad Guerfali, M.; Muller, A.; Bhat, A.H.; Abolafia, J.; Machado, R.A.R.; Kallel, S. Potential of *Oscheius tipulae* nematodes as biological control agents against *Ceratitis capitata*. *PLoS ONE* **2022**, *17*, e0269106. [CrossRef]

14. Loulou, A.; Mastore, M.; Caramella, S.; Bhat, A.; Brivio, M.; Machado, R.; Kallel, S. Entomopathogenic potential of bacteria associated with soil-borne nematodes and insect immune responses to their infection. *PLoS ONE* **2023**, *18*, e0280675. [CrossRef] [PubMed]
15. Bhat, A.H.; Loulou, A.; Abolafia, J.; Machado, R.A.R.; Kallel, S. Comparative morphological and molecular analyses of *Acrobeloides bodenheimeri* and *A. tricornis* Cobb, 1924 (Rhabditida, Cephalobidae) from Tunisia. *Nematology* **2023**, *25*, 207–226. [CrossRef]
16. Brisou, J.; Prevot, A.R. Études de systématique bactérienne. 10. Révision des espèces réunies dans le genre *Achromobacter*. In *Annales de l'Institut Pasteur*; MASSON EDITEUR: Paris, France, 1954; Volume 86, pp. 722–728.
17. Elnar, A.G.; Kim, M.-G.; Lee, J.-E.; Han, R.-H.; Yoon, S.-H.; Lee, G.-Y.; Yang, S.-J.; Kim, G.B. *Acinetobacter pullorum* sp. nov., Isolated from chicken meat. *J. Microbiol. Biotechnol.* **2020**, *30*, 526–532. [CrossRef] [PubMed]
18. Doughari, H.J.; Ndakidemi, P.A.; Human, I.S.; Benade, S. The ecology, biology and pathogenesis of *Acinetobacter* spp.: An overview. *Microbes Environ.* **2011**, *26*, 101–112. [CrossRef]
19. Li, W.; Zhang, D.; Huang, X.; Qin, W. *Acinetobacter harbinensis* sp. nov., isolated from river water. *Int. J. Syst. Evol. Microbiol.* **2014**, *64*, 1507–1513. [CrossRef]
20. Nishimura, Y.; Ino, T.; Iizuka, H. *Acinetobacter radioresistens* sp. nov. isolated from cotton and soil. *Int. J. Syst. Evol. Microbiol.* **1988**, *38*, 209–211. [CrossRef]
21. Nemec, A.; De Baere, T.; Tjernberg, I.; Vaneechoutte, M.; van der Reijden, T.J.; Dijkshoorn, L. *Acinetobacter ursingii* sp. nov. and *Acinetobacter schindleri* sp. nov., isolated from human clinical specimens. *Int. J. Syst. Evol. Microbiol.* **2001**, *51*, 1891–1899. [CrossRef]
22. Nemec, A.; Musilek, M.; Maixnerova, M.; De Baere, T.; van der Reijden, T.; Vaneechoutte, M.; Dijkshoorn, L. *Acinetobacter beijerinckii* sp nov and *Acinetobacter gyllenbergii* sp nov., haemolytic organisms isolated from humans. *Int. J. Syst. Evol. Microbiol.* **2009**, *59*, 118–124. [CrossRef]
23. Castellani, A.; Chalmers, A.J. *Manual of Tropical Medicine*, 3rd ed.; Williams Wood and Co.: New York, NY, USA, 1919.
24. van Trappen, S.; Tan, T.-L.; Samyn, E.; Vandamme, P. *Alcaligenes aquatilis* sp. nov., a novel bacterium from sediments of the Weser Estuary, Germany, and a salt marsh on Shem Creek in Charleston Harbor, USA. *Int. J. Syst. Evol. Microbiol.* **2005**, *55*, 2571–2575. [CrossRef]
25. Schroll, G.; Busse, H.-J.; Parrer, G.; Rölleke, S.; Lubitz, W.; Denner, E.B.M. *Alcaligenes faecalis* subsp. parafaecalis subsp. nov., a bacterium accumulating poly-β-hydroxybutyrate from acetone-butanol bioprocess residues. *Syst. Appl. Microbiol.* **2001**, *24*, 37–43.
26. Lu, C.-Y.; Li, Y.-Q.; Tian, Y.; Han, M.-X.; Rao, M.P.N.; Li, Y.-R.; Zhu, Z.-N.; Wei, D.-Q.; An, D.-D.; Li, W.-J. *Alcaligenes endophyticus* sp. nov., isolated from roots of *Ammodendron bifolium*. *Int. J. Syst. Evol. Microbiol.* **2017**, *67*, 939–943. [CrossRef]
27. Abbas, S.; Ahmed, I.; Kudo, T.; Iida, T.; Ali, G.M.; Fujiwara, T.; Ohkuma, M. Heavy metal-tolerant and psychrotolerant bacterium *Acinetobacter pakistanensis* sp. nov. isolated from a textile dyeing wastewater treatment pond. *Pak. J. Agric. Sci.* **2014**, *51*, 593–606.
28. Rehfuss, M.; Urban, J. *Alcaligenes faecalis* subsp. phenolicus subsp. nov. a phenol-degrading, denitrifying bacterium isolated from a graywater bioprocessor. *Syst. Appl. Microbiol.* **2005**, *28*, 421–429.
29. Hormaeche, E.; Edwards, P.R. A proposed genus *Enterobacter*. *Int. Bull. Bacteriol. Nomencl. Taxon.* **1960**, *10*, 71–74. [CrossRef]
30. Cho, G.-S.; Stein, M.; Fiedler, G.; Igbinosa, E.O.; Koll, L.P.; Brinks, E.; Rathje, J.; Neve, H.; Franz, C.M. Polyphasic study of antibiotic-resistant enterobacteria isolated from fresh produce in Germany and description of *Enterobacter vonholyi* sp. nov. isolated from marjoram and *Enterobacter dykesii* sp. nov. isolated from mung bean sprout. *Syst. Appl. Microbiol.* **2021**, *44*, 126174. [CrossRef]
31. García-González, T.; Sáenz-Hidalgo, H.K.; Silva-Rojas, H.V.; Morales-Nieto, C.; Vancheva, T.; Koebnik, R.; Ávila-Quezada, G.D. *Enterobacter cloacae*, an emerging plant-pathogenic bacterium affecting chili pepper seedlings. *Plant Pathol. J.* **2018**, *34*, 1–10. [CrossRef]
32. Wang, C.; Wu, W.; Wei, L.; Feng, Y.; Kang, M.; Xie, Y.; Zong, Z. *Enterobacter wuhouensis* sp. nov. and *Enterobacter quasihormaechei* sp. nov. recovered from human sputum. *Int. J. Syst. Evol. Microbiol.* **2020**, *70*, 874–881. [CrossRef]
33. Wu, W.; Feng, Y.; Zong, Z. *Enterobacter sichuanensis* sp. nov., recovered from human urine. *Int. J. Syst. Evol. Microbiol.* **2018**, *68*, 3922–3927. [CrossRef]
34. Wu, W.; Wei, L.; Feng, Y.; Kang, M.; Zong, Z. *Enterobacter huaxiensis* sp. nov. and *Enterobacter chuandaensis* sp. nov., recovered from human blood. *Int. J. Syst. Evol. Microbiol.* **2019**, *69*, 708–714. [CrossRef] [PubMed]
35. Xue, Y.; Hu, M.; Chen, S.; Hu, A.; Li, S.; Han, H.; Lu, G.; Zeng, L.; Zhou, J. *Enterobacter asburiae* and *Pantoea ananatis* causing rice bacterial blight in China. *Plant Dis.* **2021**, *105*, 2078–2088. [CrossRef] [PubMed]
36. Wu, W.; Feng, Y.; Zong, Z. Precise species identification for *Enterobacter*: A genome sequence-based study with reporting of two novel species, *Enterobacter quasiroggenkampii* sp. nov. and *Enterobacter quasimori* sp. nov. *Msystems* **2020**, *5*, e00527-20. [CrossRef]
37. Im, W.-T.; Yokota, A.; Kim, M.-K.; Lee, S.-T. *Kaistia adipata* gen. nov., sp. nov., a novel α-proteobacterium. *J. Gen. Appl. Microbiol.* **2004**, *50*, 249–254. [CrossRef]
38. Jin, L.; Kim, K.K.; Lee, H.-G.; Ahn, C.-Y.; Oh, H.-M. *Kaistia defluvii* sp. nov., isolated from river sediment. *Int. J. Syst. Evol. Microbiol.* **2012**, *62*, 2878–2882. [CrossRef]
39. Jin, L.; Kim, K.K.; Baek, S.-H.; Lee, S.-T. *Kaistia geumhonensis* sp. nov. and *Kaistia dalseonensis* sp. nov., two members of the class Alphaproteobacteria. *Int. J. Syst. Evol. Microbiol.* **2011**, *61*, 2577–2581. [CrossRef]
40. Lee, H.-W.; Yu, H.-S.; Liu, Q.; Jung, H.-M.; An, D.-S.; Im, W.-T.; Jin, F.-X.; Lee, S.-T. *Kaistia granuli* sp. nov., isolated from anaerobic granules in an upflow anaerobic sludge blanket reactor. *Int. J. Syst. Evol. Microbiol.* **2007**, *57*, 2280–2283. [CrossRef] [PubMed]

41. Kim, S.-J.; Weon, H.-Y.; Kim, Y.-S.; Anandham, R.; Yoo, S.-H.; Park, I.-C.; Kwon, S.-W. *Kaistia terrae* sp. nov., isolated from a wetland in Korea. *Int. J. Syst. Evol. Microbiol.* **2010**, *60*, 949–952. [CrossRef]
42. Weon, H.-Y.; Lee, C.-M.; Hong, S.-B.; Kim, B.-Y.; Yoo, S.-H.; Kwon, S.-W.; Go, S.-J. *Kaistia soli* sp. nov., isolated from a wetland in Korea. *Int. J. Syst. Evol. Microbiol.* **2008**, *58*, 1522–1524. [CrossRef]
43. Glaeser, S.P.; Galatis, H.; Martin, K.; Kämpfer, P. *Kaistia hirudinis* sp. nov., isolated from the skin of Hirudo verbana. *Int. J. Syst. Evol. Microbiol.* **2013**, *63*, 3209–3213. [CrossRef] [PubMed]
44. Orozco, R.A.; Lee, M.-M.; Stock, S.P. Soil sampling and isolation of entomopathogenic nematodes (Steinernematidae, Heterorhabditidae). *JoVE (J. Vis. Exp.)* **2014**, *89*, e52083.
45. Marchesi, J.R.; Sato, T.; Weightman, A.J.; Martin, T.A.; Fry, J.C.; Hiom, S.J.; Dymock, D.; Wade, W.G. Design and evaluation of useful bacterium-specific PCR primers that amplify genes coding for bacterial 16S rRNA. *Appl. Environ. Microbiol.* **1998**, *64*, 795–799. [CrossRef]
46. Lane, D.J. *16S/23S rRNA Sequencing*, 1st ed.; John Wiley and Sons: New York, NY, USA, 1991.
47. Hall, T. BioEdit: A user-friendly biological sequence alignment editor and analysis program for Windows 95/98/NT. In *Nucleic acids Symposium Series*; Information Retrieval Ltd.: London, UK, 1999; pp. 95–98.
48. Seemann, T. Barrnap 0.7: Rapid Ribosomal RNA Prediction. 2013. Available online: https://github.com/tseemann/barrnap (accessed on 5 June 2022).
49. Kumar, S.; Stecher, G.; Tamura, K. MEGA7: Molecular evolutionary genetics analysis version 7.0 for bigger datasets. *Mol. Biol. Evol.* **2016**, *33*, 1870–1874. [CrossRef]
50. Hasegawa, M.; Kishino, H.; Yano, T. Dating of the human-ape splitting by a molecular clock of mitochondrial DNA. *J. Mol. Evol.* **1985**, *22*, 160–174. [CrossRef]
51. Nei, M.; Kumar, S. *Molecular Evolution and Phylogenetics*; Oxford University Press: Oxford, UK, 2000; ISBN 0195350510.
52. Chevenet, F.; Brun, C.; Bañuls, A.-L.; Jacq, B.; Christen, R. TreeDyn: Towards dynamic graphics and annotations for analyses of trees. *BMC Bioinform.* **2006**, *7*, 439. [CrossRef] [PubMed]
53. Letunic, I.; Bork, P. Interactive tree of life (iTOL) v3: An online tool for the display and annotation of phylogenetic and other trees. *Nucleic Acids Res.* **2016**, *44*, W242–W245. [CrossRef]
54. Machado, R.A.R.; Bhat, A.H.; Abolafia, J.; Muller, A.; Bruno, P.; Fallet, P.; Arce, C.C.M.; Turlings, T.C.J.; Bernal, J.S.; Kajuga, J. Multi-locus phylogenetic analyses uncover species boundaries and reveal the occurrence of two new entomopathogenic nematode species, *Heterorhabditis ruandica* n. sp. and *Heterorhabditis zacatecana* n. sp. *J. Nematol.* **2021**, *53*, 1–42. [CrossRef]
55. Machado, R.A.R.; Somvanshi, V.S.; Muller, A.; Kushwah, J.; Bhat, C.G. *Photorhabdus hindustanensis* sp. nov., *Photorhabdus akhurstii* subsp. akhurstii subsp. nov., and Photorhabdus akhurstii subsp. bharatensis subsp. nov., isolated from Heterorhabditis entomopathogenic nematodes. *Int. J. Syst. Evol. Microbiol.* **2021**, *71*, 4998.
56. Petit, R.A.; Read, T.D. Bactopia: A flexible pipeline for complete analysis of bacterial genomes. *Msystems* **2020**, *5*, e00190-20. [CrossRef] [PubMed]
57. Bolger, A.M.; Lohse, M.; Usadel, B. Trimmomatic: A flexible trimmer for Illumina sequence data. *Bioinformatics* **2014**, *30*, 2114–2120. [CrossRef] [PubMed]
58. Bankevich, A.; Nurk, S.; Antipov, D.; Gurevich, A.A.; Dvorkin, M.; Kulikov, A.S.; Lesin, V.M.; Nikolenko, S.I.; Pham, S.; Prjibelski, A.D.; et al. SPAdes: A new genome assembly algorithm and its applications to single-cell sequencing. *J. Comput. Biol.* **2012**, *19*, 455–477. [CrossRef] [PubMed]
59. Walker, B.J.; Abeel, T.; Shea, T.; Priest, M.; Abouelliel, A.; Sakthikumar, S.; Cuomo, C.A.; Zeng, Q.; Wortman, J.; Young, S.K.; et al. Pilon: An integrated tool for comprehensive microbial variant detection and genome assembly improvement. *PLoS ONE* **2014**, *9*, e112963. [CrossRef] [PubMed]
60. Parks, D.H.; Imelfort, M.; Skennerton, C.T.; Hugenholtz, P.; Tyson, G.W. CheckM: Assessing the quality of microbial genomes recovered from isolates, single cells, and metagenomes. *Genome Res.* **2015**, *25*, 1043–1055. [CrossRef]
61. Price, M.N.; Dehal, P.S.; Arkin, A.P. FastTree 2–approximately maximum-likelihood trees for large alignments. *PLoS ONE* **2010**, *5*, e9490. [CrossRef]
62. Hyatt, D.; Chen, G.-L.; LoCascio, P.F.; Land, M.L.; Larimer, F.W.; Hauser, L.J. Prodigal: Prokaryotic gene recognition and translation initiation site identification. *BMC Bioinform.* **2010**, *11*, 119. [CrossRef] [PubMed]
63. Steinegger, M.; Söding, J. MMseqs2 enables sensitive protein sequence searching for the analysis of massive data sets. *Nat. Biotechnol.* **2017**, *35*, 1026–1028. [CrossRef]
64. Van Dongen, S.M. Graph Clustering by Flow Simulation [Internet]. Ph. D Thesis, University of Utrecht, Utrecht, The Netherlands, 2000.
65. van Dongen, S.; Abreu-Goodger, C. Using MCL to extract clusters from networks. In *Bacterial Molecular Networks*; Springer: Berlin/Heidelberg, Germany, 2012; pp. 281–295.
66. Katoh, K.; Standley, D.M. MAFFT multiple sequence alignment software version 7: Improvements in performance and usability. *Mol. Biol. Evol.* **2013**, *30*, 772–780. [CrossRef]
67. Stamatakis, A. RAxML-VI-HPC: Maximum likelihood-based phylogenetic analyses with thousands of taxa and mixed models. *Bioinformatics* **2006**, *22*, 2688–2690. [CrossRef]
68. Stamatakis, A. RAxML version 8: A tool for phylogenetic analysis and post-analysis of large phylogenies. *Bioinformatics* **2014**, *30*, 1312–1313. [CrossRef] [PubMed]

69. Stamatakis, A.; Hoover, P.; Rougemont, J. A rapid bootstrap algorithm for the RAxML web servers. *Syst. Biol.* **2008**, *57*, 758–771. [CrossRef] [PubMed]
70. Meier-Kolthoff, J.P.; Auch, A.F.; Klenk, H.-P.; Göker, M. Genome sequence-based species delimitation with confidence intervals and improved distance functions. *BMC Bioinform.* **2013**, *14*, 60. [CrossRef] [PubMed]
71. Meier-Kolthoff, J.P.; Hahnke, R.L.; Petersen, J.; Scheuner, C.; Michael, V.; Fiebig, A.; Rohde, C.; Rohde, M.; Fartmann, B.; Goodwin, L.A.; et al. Complete genome sequence of DSM 30083(T), the type strain (U5/41(T)) of *Escherichia coli*, and a proposal for delineating subspecies in microbial taxonomy. *Stand. Genom. Sci.* **2014**, *9*, 2. [CrossRef] [PubMed]
72. Auch, A.F.; von Jan, M.; Klenk, H.-P.; Göker, M. Digital DNA-DNA hybridization for microbial species delineation by means of genome-to-genome sequence comparison. *Stand. Genom. Sci.* **2010**, *2*, 117–134. [CrossRef]
73. Auch, A.F.; Klenk, H.-P.; Göker, M. Standard operating procedure for calculating genome-to-genome distances based on high-scoring segment pairs. *Stand. Genom. Sci.* **2010**, *2*, 142–148. [CrossRef]
74. Pan, H.; Li, J.; Liu, H.-H.; Lu, X.-Y.; Zhang, Y.-F.; Tian, Y. *Acinetobacter tibetensis* sp. nov., isolated from a soil under a greenhouse in Tibet. *Curr. Microbiol.* **2023**, *80*, 51. [CrossRef]
75. Carvalheira, A.; Gonzales-Siles, L.; Salvà-Serra, F.; Lindgren, Å.; Svensson-Stadler, L.; Thorell, K.; Piñeiro-Iglesias, B.; Karlsson, R.; Silva, J.; Teixeira, P. *Acinetobacter portensis* sp. nov. and *Acinetobacter guerrae* sp. nov., isolated from raw meat. *Int. J. Syst. Evol. Microbiol.* **2020**, *70*, 4544–4554. [CrossRef]
76. Wayne, L.G.; Brenner, D.J.; Colwell, R.R.; Grimont, P.A.; Kandler, O.; Krichevsky, M.I.; Moore, L.H.; Moore, W.E.; Murray, R.; Stackebrandt, E. Report of the ad hoc committee on reconciliation of approaches to bacterial systematics. *Int. J. Syst. Evol. Microbiol.* **1987**, *37*, 463–464. [CrossRef]
77. Lee, Y.; Jeon, C.O. *Kaistia algarum* sp. nov., isolated from a freshwater green alga *Paulinella chromatophora*. *Int. J. Syst. Evol. Microbiol.* **2018**, *68*, 3028–3033. [CrossRef]
78. Nemec, A.; Musílek, M.; Šedo, O.; de Baere, T.; Maixnerova, M.; van der Reijden, T.J.K.; Zdráhal, Z.; Vaneechoutte, M.; Dijkshoorn, L. *Acinetobacter bereziniae* sp. nov. and *Acinetobacter guillouiae* sp. nov., to accommodate *Acinetobacter* genomic species 10 and 11, respectively. *Int. J. Syst. Evol. Microbiol.* **2010**, *60*, 896–903. [CrossRef] [PubMed]
79. Kersters, K. Genus *Alcaligenes* Castellani and Chalmers 1919. *Bergey's Man. Syst. Bacteriol.* **1984**, *1*, 361–373.